# BMP Regulates Regional Gene Expression in the Dorsal Otocyst Through Canonical and Non-Canonical Intracellular Pathways

Sho Ohta[1], Baolin Wang[2], Suzanne L. Mansour[1, 3], and Gary C. Schoenwolf[1, 4]

[1]Department of Neurobiology and Anatomy, University of Utah School of Medicine, Salt Lake City, Utah.

[2]Department of Cell and Developmental Biology, and Genetic Medicine, Weill Cornell Medical College, New York, New York.

[3]Department of Human Genetics, University of Utah School of Medicine, Salt Lake City, Utah.

[4]Address correspondence to: **Schoenwolf@neuro.utah.edu**.

**Keywords:** Dorsalization, Inner Ear, Otocyst, Polarization, Signaling

**Abstract**

The inner ear consists of two otocyst-derived, structurally and functionally distinct components: the dorsal vestibular and ventral auditory compartments. BMP signaling is required to form the vestibular compartment, but how it complements other required signaling molecules and acts intracellularly is unknown. Using spatially and temporally controlled delivery of signaling pathway regulators to developing chick otocysts, we show that BMP signaling regulates expression of *Dlx5* and *Hmx3*, both of which encode transcription factors essential for vestibular formation. However, while BMP regulates *Dlx5* through the canonical SMAD pathway, surprisingly, it regulates *Hmx3* through a non-canonical pathway involving both an increase in cAMP-dependent protein kinase A activity and the GLI3R to GLI3A ratio. Thus, both canonical and non-canonical BMP signaling establish the precise spatiotemporal expression of *Dlx5* and *Hmx3* during dorsal vestibular development. The identification of the non-canonical pathway suggests an intersection point between BMP and SHH signaling, which is required for ventral auditory development.

## Introduction

The inner ear is a morphologically complex three-dimensional organ with regionally specified sensory functions. It develops from the otocyst, an initially spherical epithelial primordium that forms adjacent to the caudal hindbrain. Growth factors secreted from neighboring structures, such as the neural tube and notochord, establish the dorsoventral (DV) patterning of the otocyst (Bok et al., 2007a; Groves and Fekete, 2012; Riccomagno et al., 2002; Riccomagno et al., 2005; Wu and Kelley, 2012). Two signaling systems, Wingless-type MMTV integration site family (WNT) and Sonic hedgehog (SHH), play particularly important roles in this process. Each is presumed to provide positional information across the DV axis of the otocyst by forming concentration gradients; namely, a dorsal-high to ventral-low gradient of WNT that patterns mainly the dorsal otocyst, and an opposing gradient of SHH that patterns mainly the ventral otocyst (Bok et al., 2005; Bok et al., 2007a; Ohyama et al., 2006; Riccomagno et al., 2002; Riccomagno et al., 2005). *Wnt1* and *Wnt3a* expressed in the dorsal neural tube, but not in the otocyst, are required for vestibular development (Riccomagno et al., 2005). SHH signaling, in contrast to WNT signaling, patterns the ventral otocyst and is required for formation of the cochlear duct. Absence of SHH signaling in $Shh^{-/-}$ mutant mouse embryos, or ablation of the embryonic tissue secreting SHH (notochord and floor plate of the neural tube) in chick embryos, results in complete loss of the cochlear duct (Bok et al., 2005; Bok et al., 2007b; Brown and Epstein, 2011; Riccomagno et al., 2002).

SHH signaling is mediated by GLI transcription factors, of which there are two functionally distinct types: activators (GLIA) and repressors (GLIR) (Briscoe and Novitch, 2008; Ingham and McMahon, 2001). cAMP-dependent protein kinase A (PKA) phosphorylates full-length GLI, stimulating its proteolytic processing to GLIR (Chen et al., 1998; Wang et al., 2000). During development of the inner ear, GLI2 and GLI3 play crucial roles in mediating SHH signaling through their dual functions. In the ventral otocyst, which is closest to the source of SHH signaling, the unprocessed GLIA forms are expected to predominate, whereas in the dorsal otocyst, which is distant from the source of SHH signaling, partial proteolytic processing of the full-length form is expected to occur, generating the GLIR forms. Based on the analysis of mouse *Gli* mutant embryos, it was suggested that formation of the cochlear duct requires predominantly GLI2A and GLI3A, whereas formation of the vestibular system requires predominantly GLI3R (Bok et al., 2007a).

Although a simple model of otocyst DV patterning is appealing, in which opposing gradients of only two signaling pathways are required, other evidence suggests that patterning is more complex. For example, in the absence of SHH signaling, *Dlx5*, a gene normally

expressed in the dorsal otocyst, is expanded ventrally; however, another dorsally expressed gene, *Hmx3* (formerly called *Nkx5.1*), is unaffected (Riccomagno et al., 2002). Moreover, *Pax2* and *Otx2*, two genes expressed in the ventral otocyst, are expressed normally in the *Wnt1/Wnt3a* double mutant, rather than being expanded dorsally (Riccomagno et al., 2005). These results suggest that other signals in addition to WNTs and SHH provide regional information for otocyst DV patterning. Among possible candidates are BMPs. BMPs are expressed in the roof plate of the hindbrain and in the adjacent dorsomedial margin of the otic cup (Oh et al., 1996; Wu and Oh, 1996), as well as within the wall of the dorsal otocyst itself (Chang et al., 2008; Oh et al., 1996; Wu and Oh, 1996). Chromatography beads coated with the BMP antagonist, Noggin, and implanted into chick embryos adjacent to the dorsal otocyst inhibit formation of the semicircular canals (Chang et al., 1999; Gerlach et al., 2000). Similarly, conditional knock out of *Bmp4* in the developing mouse inner ear results in loss of the three sensory cristae and their associated semicircular canals, whereas the cochlear duct seems unaffected (Chang et al., 2008). Thus, in addition to WNT signaling, BMP signaling is required for development of dorsal otocyst structures.

In the dorsolateral otocyst, BMP signaling was suggested to maintain, either directly or indirectly, expression of two homeobox genes, *Dlx5* and *Hmx3,* which are transcription factors required to form the primordial canal pouch (Hadrys et al., 1998; Merlo et al., 2002; Wang et al., 2004; Wang et al., 1998). However, it is unknown how BMP signaling molecularly regulates the expression of these genes.

Here, we show that BMP signaling regulates both *Dlx5* and *Hmx3* expression in the dorsal otocyst and this occurs through distinct intracellular pathways. Specifically, the canonical pSMAD pathway regulates *Dlx5* expression, whereas a non-canonical pathway that activates PKA and increases the ratio in the dorsal otocyst of GLI3R to GLI3A regulates *Hmx3*. Thus, both canonical and non-canonical BMP signaling are important for dorsal otocyst patterning, and the non-canonical pathway suggests a link that could be used to coordinate dorsal and ventral otocyst patterning signals.

## Results

### Gain of BMP signaling inhibits cochlear duct development and induces *Hmx3* and *Dlx5* expression

Previous loss-of-function studies showed that BMPs are required to form the vestibular system (Chang et al., 2008; Chang et al., 1999; Chang et al., 2002; Gerlach et al., 2000; Ohta et al., 2010). However, whether increasing BMP signaling dorsalizes the early otocyst is unknown. To determine this, we co-sonoporated *Bmp4* and *Gfp* into the ventral head mesenchyme of chick embryos at HH stages 9-11 (Fig. 1A-C). Computer-aided 3D reconstruction of the inner ears 5-6 days later showed that in comparison with the control side, development of the cochlear duct on the sonoporated side was strongly inhibited, whereas both the vestibular system and endolymphatic duct were normal (Fig. 1D-F). Moreover, 60 hours after sonoporation, the expression of two transcription factors normally restricted mainly to the dorsal otocyst, *Hmx3* and *Dlx5,* were altered. Relative to embryos treated with *Gfp* only, the expression of both genes was expanded ventromedially within the otocyst of embryos treated with both *Bmp4* and *Gfp* (Fig. 1G-J; plus signs). Moreover, expression of *Otx2*, a gene normally expressed ventrally in the nascent cochlear duct, was inhibited (Fig. 1K,L; negative signs). Thus, these results show that gain-of-BMP signaling ventrally is sufficient to dorsalize the ventral otocyst, suggesting that BMP signaling plays a role in establishing dorsal polarity of the otocyst.

### Loss of BMP signaling inhibits dorsal otocyst development and attenuates *Hmx3* and *Dlx5* expression while expanding *Otx2* expression dorsally

Previously, we reported that overexpression of *Noggin*, a BMP antagonist, resulted in the complete loss of the three semicircular canals 5-6 days later, whereas the endolymphatic duct and cochlear duct formed essentially normally (Ohta et al., 2010). To further test the requirement of BMP signaling in patterning the dorsal otocyst, we blocked BMP signaling again by co-sonoporating *Noggin* and *Gfp* into the dorsal head mesenchyme of chick embryos at HH stages 15-16 (Fig. 2A-C). First, we confirmed our previous result, once more showing the loss of the semicircular canals and the persistence of the endolymphatic duct and cochlear duct (Fig. 2D). Then, we asked whether BMP signaling is required for *Hmx3* and *Dlx5* expression in the dorsal otocyst. In otocysts treated with *Noggin* and *Gfp,* formation of the primordial canal pouch was inhibited 48 hours later, and both *Hmx3* and *Dlx5* expression was greatly diminished (Fig. 2E-H; black arrowheads), with the exception that *Dlx5* was still expressed in the forming endolymphatic duct (Fig. 2H, red arrowhead). Moreover, *Otx2*

expression was expanded dorsally (Fig. 1I,J; red arrowheads) and was even expressed ectopically in the most dorsal otocyst cells (Fig. 1J; asterisk, inset). These results show that BMP signaling is required for both *Hmx3* and *Dlx5* expression, and that it restricts *Otx2* expression to the ventral otocyst.

**BMP signaling controls *Dlx5* expression through the pSMAD pathway**

To determine whether BMP signaling controls *Hmx3* and/or *Dlx5* expression in the dorsal otocyst through its canonical pathway, we blocked pSMAD signaling in the dorsal otocyst by co-electroporating the inhibitory SMAD, *Smad6*, and *Gfp* into the dorsolateral wall of the otocyst at HH stages 15-16 (Fig. 3A-C). Twelve hours later, pSMAD labeling was still present in the dorsal region of control otocysts transfected with *Gfp* alone (Fig. 3D,d), but in otocysts co-transfected with *Smad6* and *Gfp,* pSMAD labeling in the dorsal otocyst was absent (Fig. 3E,e), confirming that overexpression of *Smad6* blocked pSMAD signaling. Additionally, co-transfection of *Smad6* and *Gfp* into the dorsal otocyst completely inhibited development of the semicircular canals, but development of the endolymphatic duct and cochlear duct were essentially unaffected (Fig. 3F,G).

We next examined *Hmx3* and *Dlx5* expression in the otocyst at HH stages 20-21. Neither *Dlx5* nor *Hmx3* expression was affected after treatment with *Gfp* alone (Fig. 3H-k). However, after treatment with *Smad6* and *Gfp*, *Dlx5* expression was abolished dorsolaterally (Fig. 3I,i), with the exception that cells in the dorsomedial otocyst (i.e., those that form the endolymphatic duct) still expressed *Dlx5* (Fig. 3I,I''). In striking contrast, all treated otocysts still expressed *Hmx3* (Fig. 3J-k). These results clearly show that BMP signaling regulates *Dlx5* expression in the dorsolateral otocyst through the canonical pSMAD pathway, whereas *Hmx3* expression is not regulated by this pathway, suggesting a role for a non-canonical BMP signaling pathway.

**BMP signaling controls *Hmx3* expression through a non-canonical pathway that involves GLI3 protein processing**

Analysis of inner ear phenotypes in *Gli* mutant mice suggested that GLIR and GLIA are present in the early otocyst as reciprocal dorsoventral (DV) protein gradients, with repressor being high dorsally and activator high ventrally (Bok et al., 2007a). This raises the possibility that such a gradient might control *Hmx3* expression in the dorsolateral otocyst. To test this, we co-electroporated *Gli3R* and *Gfp* into the ventral otic epithelium of chick embryos at HH stages 9-11 (Fig. 4A-C) to alter the gradient, counteracting the higher level of *Gli3A* expected

to be present in the ventral otocyst, and examined gene expression 24-30 hours later at HH stages 20-21. In control otocysts transfected with *Gfp* alone, *Hmx3* expression was unaltered (Fig. 4D,d), but in otocysts co-transfected with *Gli3R* and *Gfp*, ectopic *Hmx3* expression occurred ventromedially (Fig. 4E,e). Additionally, *Dlx5* expression was unchanged in both control (Fig. 4F,f) and *Gli3R*-transfected otocysts (Fig. 4G,g). Thus, GLI3 signaling controls *Hmx3* expression in the otocyst, but not *Dlx5* expression.

To ask whether BMP signaling regulates GLI3FL proteolytic processing to increase the level of GLI3R, we altered the level of BMP signaling. Either *Bmp4* or *Noggin* was co-sonoporated with *Gfp* as described above (Fig. 1A, 2A). Otocysts were collected 48-60 hours later, when they reached HH stages 24-25, and pooled for western blotting to detect GLI3 (Wang et al., 2000). After overexpression of *Bmp4* and *Gfp*, the ratio of GLI3R to GLI3FL in otocysts was 1.8 times greater than that of control otocysts due to an increase in GLI3 processing (i.e., an increase in GLI3R; Fig. 4H,H'). In contrast, after overexpression of *Noggin* and *Gfp*, the ratio was dramatically decreased due to a reduction in GLI3R (Fig. 4I,I'). These results provide strong evidence that BMP signaling plays an important role in GLI3FL protein processing to increase the level of GLI3R. In addition, we asked whether BMP signaling through its pSMAD pathway affects GLI3FL processing. *Smad6* and *Gfp* were co-electroporated into the dorsolateral otocyst as described above (Fig. 3A). Otocysts were again collected 24-30 hours later when embryos reached HH stages 24-25 and pooled for western blotting to detect GLI3. The GLI3R/GLI3FL ratio was unchanged, showing that the canonical BMP/pSMAD pathway does not participate in GLI3FL processing (Fig. 4J,J').

**BMP signaling affects PKA activity, and increasing PKA activity inhibits cochlear duct development and induces *Hmx3* expression, but not *Dlx5* expression**

GLI3FL is phosphorylated by PKA, stimulating the proteolytic processing of GLI3FL to GLI3R (Chen et al., 1998; Wang et al., 2000). Thus, we next asked whether BMP signaling upregulates PKA activity. To do this, either *Bmp4* or *Noggin* was co-sonoporated along with *Gfp* as described above (Fig. 1A, 2A). Otocysts were collected 48-60 hours later when embryos reached HH stages 24-25 and pooled for PKA activity assays. *Bmp4* and *Gfp* overexpression increased PKA activity in the otocyst by more than 40% (Fig. 5A). In concert with this, *Noggin* and *Gfp* overexpression decreased PKA activity by more than 50% (Fig. 5B). These results suggest that BMP signaling affects PKA activity in the developing otocyst.

We next asked whether increased PKA activity affects GLI3FL proteolytic processing in the otocyst. To do this, we co-electroporated the ventral otic epithelium, as described

previously (Fig. 4A), with constitutively active PKA (ca*Pka*) and *Gfp*. Otocysts were collected 24-30 hours later when they reached HH stages 20-21 and pooled for western blotting to detect GLI3. Overexpression of ca*Pka* and *Gfp* resulted in an increased GLI3R/GLI3FL ratio due to excess production of GLI3R (Fig. 5C,C'). This suggests that PKA activity can regulate GLI3FL proteolytic processing, thereby changing the DV ratio of GLI3FL/R in the otocyst.

Computer-aided 3D reconstruction of inner ears 5-6 days after ca*Pka* transfection showed that the cochlear duct was severely truncated, whereas the vestibular system and endolymphatic duct were normal (Fig. 5D-F), suggesting that increased PKA activity dorsalizes the ventral otocyst by altering regional gene expression. To address this, we transfected HH stage 9-11 otocysts ventrally (Fig. 4A) with ca*Pka* and *Gfp,* and 24-30 hours later assessed *Hmx3* and *Dlx5* expression in otocysts at HH stages 20-21. In otocysts transfected with *Gfp* alone, *Hmx3* expression was unaffected (Fig. 5G,g), but in otocysts co-transfected with ca*Pka* and *Gfp, Hmx3* was ectopically expressed in ventral cells (Fig. 5H,h). In contrast, *Dlx5* expression was unaffected in otocysts transfected with *Gfp* alone (Fig. 5I,i) or after co-transfection with ca*Pka* and *Gfp* (Fig. 5J,j). These results suggest that *Hmx3* expression, but not *Dlx5* expression, is regulated during dorsal patterning of the otocyst by a non-canonical BMP signaling pathway. Moreover, our results suggest that the non-canonical pathway involves the activation of PKA and increased GLI3 proteolytic processing,

**Inhibition of ventral otocyst development by ca*Pka* is rescued with ca*Gli3A* (*Gli3A$^{HIGH}$*)**

To determine whether ca*Pka* overexpression inhibited development of the cochlear duct specifically by increasing the level of GLI3R, we attempted to rescue ventral otocyst development after ca*Pka* overexpression by co-expressing ca*Gli3A* (*Gli3A$^{HIGH}$*). ca*Gli3A* acts as a constitutively active transcriptional activator (Stamataki et al., 2005), so we expected that ca*Gli3A* would counteract the elevated GLI3R in the ventral otocyst that resulted from the increased PKA activity. pCAß-IRES-*Gfp* vector alone, pCAß-ca*Pka*- IRES-*Gfp,* or pCAß-ca*Pka*-IRES-*Gfp* and pCAGGS-ca*Gli3A* was electroporated into the ventromedial the otocyst and embryos were collected 60 hours later for in situ hybridization with *Otx2* or 72 hours later for computer-aided serial section reconstruction (Fig. 6A-I). As expected, *Otx2* expression was unchanged after overexpression of vector alone (Fig. 6A) and the otocyst developed normally (Fig. 6B,C). Also as expected, *Otx2* expression was essentially absent after overexpression of ca*Pka* (Fig. 6D) and development of the cochlear duct was inhibited (Fig. 6E,F). In contrast, co-overexpression of ca*Pka* and ca*Gli3A* (plus *Gfp*) restored virtually

normal *Otx2* expression (Fig. 6G) and cochlear duct development (Fig. 6H,I). Measurements of the cochlear duct showed that its length was not statistically different between control and rescued ducts, but that it differed statistically between control and ca*Pka*-treated ducts, as well as between ca*Pka*-treated and rescued ducts (Fig. 6J). Collectively, these results provide strong evidence that overexpression of ca*Pka* inhibited development of the cochlear duct specifically by increasing the level of GLI3R.

## Discussion

DV patterning of the otocyst involves the secretion of WNTs from the dorsal hindbrain and SHH from the notochord and floor plate of the hindbrain (Groves and Fekete, 2012; Wu and Kelley, 2012). In addition, considerable evidence supports an obligatory role for BMP signaling in dorsalization of the inner ear (Chang et al., 2008; Chang et al., 2002; Gerlach et al., 2000; Ohta et al., 2010). Here, we show that BMP signaling is essential for establishing otocyst dorsal polarity, and that at least two intracellular pathways are involved: a canonical pSMAD1/5/8 pathway and a non-canonical pathway that activates PKA and increases the GLI3R/FL ratio by increasing the amount of GLI3R present in the dorsal otocyst. These two BMP-regulated pathways coordinate dorsalization of the otocyst, inducing expression of both *Dlx5* and *Hmx3*, transcription factors essential for normal formation of the vestibular system (Fig. 7).

### Interplay between dorsal signaling factors during inner ear development

In TOPGAL mouse embryos, ßGAL is detected in the dorsomedial portion of the otic epithelium, the region of the otocyst closest to the dorsal neural tube, the site of WNT secretion. Additionally, in tissue explants from such embryos, both ßGAL and *Dlx5* respond in a dose-dependent manner to WNT/ß-catenin signaling by expanding their expression ventrally in the otocyst (Riccomagno et al., 2005). These data clearly indicate that the dorsal otocyst responds to WNT signaling.

We showed previously that the BMP-effector pSMAD1/5/8 is localized to the dorsolateral otocyst (Ohta et al., 2010), suggesting that BMPs also pattern the dorsal otocyst. When we inhibited BMP signaling using reagents that presumably would not inhibit WNT signaling (namely, *Noggin* or *Smad6*), the semicircular canals were partially or completely lost and expression of some dorsal otocyst genes was inhibited (e.g., both *Hmx3* and *Dlx5* with *Noggin*, and only *Dlx5* with *Smad6*). These results show that BMP signaling, like WNT signaling, is required to pattern the dorsal otocyst, and that neither growth factor alone is

sufficient to effect full dorsal patterning. Moreover, in *Wnt1*$^{-/-}$;*Wnt3a*$^{-/-}$ double mutant mouse embryos, the size of the otocyst is severely reduced, but *Bmp4* expression persists in the dorsolateral epithelium of the otocyst (Riccomagno et al., 2005), suggesting that the otocyst still receives BMP signals in these embryos. Nevertheless, these mutant embryos have severely disrupted inner ears lacking vestibular components. Thus, both WNT and BMP signaling are required for dorsal patterning of the otocyst and proper formation of the vestibular system.

**Regulation of *Dlx5* expression in the dorsolateral otocyst by canonical BMP signaling**

In the early otocyst, *Dlx5* is expressed throughout the forming semicircular canals and endolymphatic duct (Brown et al., 2005). At later stages, expression of *Dlx5* in the canals becomes restricted to their nonsensory regions in a pattern complementary to that of their sensory patches, which express *Bmp4*; thus, *Dlx5* and *Bmp4* are expressed in discrete, non-overlapping regions (Brown et al., 2005). *Dlx5* null mutant embryos have severe defects in the dorsal otocyst, lacking all three semicircular canals and forming a truncated endolymphatic duct (Merlo et al., 2002). Therefore, *Dlx5* plays an essential role in formation of the dorsal otocyst.

In the present study, we showed that inhibition of canonical BMP signaling blocked *Dlx5* expression. However, as mentioned above, *Dlx5* expression is regulated in a dose-dependent manner by WNT/β-catenin signaling (Riccomagno et al., 2005). In addition, conditional inactivation of β-catenin in the otic placode of mouse embryos results in a dramatic reduction of *Dlx5* expression, whereas conditional activation of the canonical WNT pathway causes an expansion of *Dlx5* expression (Ohyama et al., 2006). Thus, it seems that the spatiotemporal pattern of *Dlx5* expression in the developing inner ear is regulated by at least two pathways, both canonical BMP signaling and canonical WNT signaling. As mentioned above, *Dlx5* is broadly expressed in the entire dorsal otocyst, including its dorsomedial region, which forms the endolymphatic duct, and its dorsolateral region, which forms the semicircular canals. *Dlx5* expression in the dorsolateral region of the otocyst, a region that is relatively far from the dorsal neural tube, the source of WNT signaling, is likely to be regulated by BMP signaling, whereas *Dlx5* expression in the dorsomedial region is likely to be regulated by WNT signaling, at least in part. Consistent with this, we showed that inhibition of BMP signaling in the otic epithelium reduced *Dlx5* expression in the dorsolateral region but not in the dorsomedial region. Similar results also occurred in otic conditional *Bmp4* knockout mice, in which *Dlx5* expression is reduced in the canal pouch, but not more medially in the

endolymphatic duct (Fig. 3I in Chang et al., 2008). Thus, coordination of the two pathways is necessary for precise spatiotemporal expression of *Dlx5* during vestibular development.

**Regulation of *Hmx3* expression in the dorsolateral otocyst by non-canonical BMP signaling**

*Hmx3* and *Hmx2* (previously called *Nkx5.1* and *Nkx5.2,* respectively) genes are expressed in the dorsolateral otocyst where they almost completely overlap with the *Dlx5* expression domain (Herbrand et al., 1998). Disruption of either or both of the *Hmx* genes gives rise to a phenotype similar to that of the *Dlx5* mutant, that is, absence of the semicircular canals (Hadrys et al., 1998; Merlo et al., 2002; Wang et al., 2004; Wang et al., 1998). Both *Dlx5* and *Hmx3* play crucial roles in formation of the vestibular system (Merlo et al., 2002). However, *Hmx3* expression seems to be regulated by a pathway that is distinct from that of *Dlx5*. As mentioned above, *Dlx5* expression in the dorsal otocyst is likely regulated by both WNT and BMP signaling. However, *Hmx3* expression is unlikely to require WNT signaling, as disruption of *Wnt1* and *Wnt3a,* or ablation of the dorsal neural tube, does not affect *Hmx3* expression (Riccomagno et al., 2005). Intriguingly, when we blocked BMP signaling with *Noggin, Hmx3* expression in the dorsolateral otocyst was attenuated but still present, whereas *Dlx5* expression was almost extinguished. This suggests that regulation of *Hmx3* expression is less sensitive to loss of BMP signaling than is *Dlx5* expression. Similar results were obtained in *Bmp4* conditional knockout mice, namely, strongly reduced *Dlx5* expression in the dorsolateral otocyst, with persisting, but apparently weaker, *Hmx3* expression (Chang et al., 2008). Collectively, these results indicate that BMP signaling alone is not sufficient to regulate full expression of *Hmx3* in the dorsolateral otocyst.

In the current study, we showed that gain of GLI3R function in the otocyst induced ectopic expression of *Hmx3*, suggesting that GLI3R is a key factor positively regulating *Hmx3* expression. This finding raises the question of what signaling pathways lead to the production of GLI3R. At least two pathways may be involved. One is the SHH pathway. According to an existing model of DV inner ear patterning (Bok et al., 2007a), the dorsal region of the otocyst should have a high concentration of GLI3R, as compared to the ventral region, because it should receive considerably less (or no) SHH signaling, which is generated from axial tissues ventral to the otocyst (Hui and Angers, 2011). Consistent with this, *ShhP1* transgenic mouse embryos, which have ectopic SHH expression in the dorsal otic epithelium, have decreased *Hmx3* expression (Riccomagno et al., 2002). Although not assessed by the authors in their study, we would expect that increased dorsal signaling of SHH would lead to

a decrease in GLI3R dorsally. A second possible signaling pathway to regulate GLI3R is the non-canonical BMP pathway revealed in the current study. This pathway mediates PKA activation, which phosphorylates GLI3FL and results in production of GLI3R. Presumably, the higher amount of GLI3R maintained in the dorsal otocyst by both lack of SHH signaling and active non-canonical BMP signaling would be necessary to induce the appropriate level of *Hmx3* expression required for normal vestibular development.

**Model: Molecular pathways regulating *Dlx5* and *Hmx3* expression in the developing otocyst**

Our results show that canonical BMP signaling regulates *Dlx5* expression in the dorsolateral otocyst (Fig. 7). Inhibition of SMAD signaling with *Smad6* almost completely abolishes *Dlx5* expression, whereas *Dlx5* expression in the dorsomedial otocyst, including the endolymphatic duct, was not affected. Previous reports suggest that the *Gbx2* homeobox gene is also involved in regulating *Dlx5* expression. *Gbx2* mutant mice lack *Dlx5* expression in the dorsomedial domain of the otocyst, but expression in the dorsolateral domain persists (Lin et al., 2005). Moreover, WNT and FGF signaling have been suggested to play a role in inducing and maintaining *Gbx2* expression, which in turn induces *Dlx5* expression (Hatch et al., 2007; Riccomagno et al., 2005).

Our results also show that *Hmx3* expression is ectopically induced in the ventral otocyst by gain of Gli3R function, suggesting that the function of GLI protein (i.e., as an activator or repressor) along the dorsoventral axis of the otocyst regulates *Hmx3* expression (Fig. 7). According to a model proposed by Wu and colleagues, the dorsal region of otocyst would be expected to have a high dose of GLI repressor due to the absence (or low level) of SHH signaling occurring there (Bok et al., 2007a). Moreover, our results suggest that non-canonical BMP signaling increases PKA activity, which in turn would be expected to phosphorylate GLI3FL, resulting in its partial proteolysis and the production of GLI3R. Our rescue experiments strongly support this expectation. Collectively, our results suggest that the regulation of *Hmx3* expression in the dorsolateral otocyst involves GLI3R-maintained crosstalk between SHH and BMP signaling.

**A possible molecular pathway mediating PKA activation by BMP non-canonical signaling**

Several studies have reported that BMP signaling can upregulate PKA activity (Gangopahyay et al., 2011; Lee and Chuong, 1997; Liu et al., 2005; Tee et al., 2010). However, the molecular pathway by which this occurs remains unclear. Because binding of cAMP(s) to the regulatory subunit(s) of PKA is thought to be indispensable for activation of PKA (Granot et al., 1980; Taylor et al., 1990), BMP signaling presumably interacts directly or indirectly with a G-protein-coupled-receptor (GPCR) to increase the production of intracellular cAMP. The parathyroid hormone (PTH)/PTH-related protein (PTHrP) pathway is a likely one with potential to interact with BMP to control cAMP production. The PTH/PTHrP receptor can activate the $G_{\alpha s}$ subunit that activates the adenylate cyclase (AC)/PKA pathway in a ligand-dependent manner (Fujimori et al., 1992). Numerous reports have suggested that BMP signaling directly or indirectly regulates bone development by interacting with the PTH/PTHrP pathway (Minina et al., 2001; Susperregui et al., 2008; Zou et al., 1997). In the developing inner ear, *PTHrP* seems to be expressed in its dorsal epithelial wall, including the semicircular canals, but not in the endolymphatic duct, and it is also expressed in mesenchyme surrounding the cochlear duct (Karperien et al., 1996; Lee et al., 1995). In contrast, *PTH receptor* is diffusely expressed in both the inner ear epithelium and surrounding mesenchyme (Lee et al., 1995). Albright's hereditary osteodystrophy, a human congenital disease characterized by the inability to respond to PTH, involves hearing loss in some patients (Wilson and Trembath, 1994), but whether vestibular development is also affected is unknown. Although these results raise the possibility that the PTHrP pathway may function in BMP signaling in the inner ear, further studies are needed to directly test this.

## Materials and methods

### Embryos

Fertilized White Leghorn chick eggs were incubated at 38.5°C until embryos reached desired stages (Hamburger and Hamilton, 1951).

### Western blotting

Otocysts were manually dissected from chick embryos at HH stages 20-24, pooled (5-20 for each lane), digested with dispase (GIBCO: 0.5 U/ml for 30-45 minutes at 37°C), and lysed with ice-cold RIPA buffer. Protein concentration was measured using the Pierce Coomassie Plus Bradford Assay Kit (ThermoFisher). Equal amounts of protein were loaded onto 7.5% SDS-PAGE gels, and western blotting was performed with GLI3 antibody as described previously (Pan and Wang, 2007; Wang et al., 2000). A monoclonal antibody to α-tubulin (1:2000, Sigma T6199) was used as a loading control. Secondary antibodies consisted of mouse IgGs conjugated with HRP (GE Healthcare, NA9310V).

### Gene transduction

Electroporation was used to deliver genes encoding intracellular proteins to discrete, selected regions of the wall of the otocyst, and sonoporation was used to deliver genes encoding extracellular proteins to mesenchymal cells either directly ventral to the otic placode or dorsal to the otocyst. Chick eggs were windowed using standard techniques, the vitelline membranes were removed, the amnion (at stages when present) was opened over the otocyst, and embryos were either sonoporated (Ohta et al., 2003) or electroporated (Ohta et al., 2010) *in ovo* to transfect expression vectors. For sonoporation, a DNA-microbubble mixture was prepared by adding 10 µl of a plasmid DNA solution (concentration 2.0-4.0 µg/µl) to 10 µl of SonoVue (BRACCO), and the mixture was injected into the head mesenchyme adjacent to the otocyst using a glass micropipette (GD-1.2, Narishige). Stages were selected to target sonoporation ventrally (HH stages 9-11; Fig. 1A) or dorsally (HH stages 15-16; Fig. 2A). Injected embryos were immediately exposed to ultrasound using a 3-mm diameter probe (Sonitron 2000N, Nepagene) with an input frequency of 1 MHz, an output intensity of 2.0 W/cm$^2$, and a pulse duty ratio of 20% for 60 sec. Embryos were usually collected after an additional 48-60 hours upon reaching HH stages 24-25.

For electroporation, the plasmid solution (2.0 μg/μl) contained 0.1% fast green for visualization, and was injected into the lumen of the developing otocyst (or cavity of the otic cup) using a glass micropipette. Stages were selected to target electroporation to the dorsolateral (HH stages 15-16; Fig. 3A) or ventromedial (HH stages 9-11; Fig. 4A) otocyst wall, and electrodes were positioned accordingly. In HH stage 9-11 embryos, the positive electrode was placed in the subcephalic pocket beneath the otic placode and the negative electrode was placed just above (dorsal to) the placode. In HH stage 15-16 embryos, the negative electrode was inserted into the otocyst lumen through the nascent endolymphatic duct and the positive electrode was placed just above (lateral to) the otocyst. Needle electrodes were used exclusively (tungsten, diameter 0.010 inch, length 3 inches, tapered tip of 12°, and AC resistance = 5 M ohms) and were purchased from A-M Systems (Sequim, WA; catalog no., 577300). Two 50-msec pulses at 10 volts were applied using a CUY21 electroporator (Nepa Gene). Embryos were usually collected 18-36 hours later upon reaching HH stages 20-21.

For rescue experiments, the plasmid mixture was prepared by adding 2 μl of pCAβ-ca*Pka*-IRES-*Gfp* (concentration 0.5 μg/μl) to 2 μl of pCAGGS-ca*Gli3A*(*Gli3A*$^{HIGH}$) (concentration 0.5 μg/μl) and electroporated into the ventromedial wall of the otocyst in chick embryos at HH stages 9-11. Non-rescued but experimentally treated otocysts were electroporated with pCAβ-ca*Pka*-IRES-*Gfp* (concentration 0.5 μg/μl) alone.

**Expression vectors**

pCAGGS-*Gfp* was obtained from H. Ogawa (Ogawa et al., 1995) and pCAGGS-*Gli3A*$^{HIGH}$ and pCAGGS-*Gli3R* were obtained from J. Briscoe (Stamataki et al., 2005). pCAGGS-m*Bmp4* was described previously (Ohta et al., 2003). Full-length mouse *Noggin* cDNA was obtained from A. McMahon and inserted into a pCAGGS vector. pCS2-h*Smad6* was purchased from Addgene (plasmid 14960). The constitutively active catalytic subunit of protein kinase A (PKA) was isolated from an RCAS(A) vector (from A. Munsterberg) using a ClaI site and subcloned into a ClaI site of pCAβ-IRES-*Gfp* (from A. Tucker).

**Three-dimensional visualization of inner ear**

Inner ear morphology was visualized in two ways. First, paraffin serial transverse sections of chick embryos at stages 30-35 were stained with hematoxylin and eosin, photographed, and reconstructed three-dimensionally using Amira 5.1 software (FEI). Second, the otocyst lumen was filled with white paint, as described previously (Morsli et al., 1998), to create a cast of the otocyst's three-dimensional shape. Phenotypes were readily detectable in serial sections, but computer-aided reconstructions and paint fills are shown in the figures to aid visualization of the inner ear's complex 3D morphology.

**PKA activity assay**

Dissected otocysts from embryos at HH stages 24-25 were pooled (20 per run), enzymatically digested as described above, and lysed in buffer consisting of 25mM Tris-HCl (pH 7.4), 0.5 mM EDTA, 0.5mM EGTA, and 10 mM β-mercaptoethanol, with one inhibitor cocktail tablet (Complete, Roche) added per 50 ml. PKA activity was measured using a PepTag kit (Promega).

**ISH hybridization on paraffin sections**

Chick embryos were fixed with 4% paraformaldehyde and embedded in paraffin, and transverse sections were subjected to ISH using standard procedures with chick (c) probes for c*Hmx3*, c*Dlx5*, and c*Otx2* (from, respectively, Drs. E. Bober, W. Upholt, and L. Bally-Cuif).

**Immunolabeling**

Transfected cells were detected in transverse paraffin sections with a monoclonal primary antibody against GFP (Roche, 11814460001). pSMAD1/5/8 (Cell Signaling Technology, #9511) was detected with a rabbit polyclonal antibody, diluted 1:200 in blocking solution (0.1% sheep serum). Secondary antibodies conjugated to AlexaFluor 488 or AlexaFluor 594 were diluted to 1:1000 (Invitrogen, A21202 and A11012, respectively) and imaged using an Olympus microscope.

**Statistical analysis**

Sample size was based on past, similar experiments and feasibility. Statistical analyses were performed using Minitab Express (Minitab). In each experiment, we used the Anderson-Darling test to evaluate whether the data fit a normal distribution, and the F-test to examine whether variances between the two groups (control and experiment) were similar. Based on

this, means and standard derivations were calculated and shown in the graphs, with *P*-values obtained using a two-tailed, unpaired Student's t-test. When more than two groups were compared (Fig. 6J), means were compared statistically with the one-way ANOVA test.

**Acknowledgments**

Yukio Saijoh and Lisa Urness provided critical comments. Research reported in this publication was supported by the National Institute on Deafness and Other Communication Disorders of the National Institutes of Health under award number DC01819. The content is solely the responsibility of the authors and does not necessarily represent the official views of the National Institutes of Health.

**Author Contributions**

Sho Ohta: Conceived and executed all experiments, analyzed all data, and drafted the manuscript.

Baolin Wang: Provided reagents and helped with experimental design, and provided input on the manuscript.

Suzanne L. Mansour: Provided input on experiments and data interpretation and edited the manuscript.

Gary C. Schoenwolf: Assisted in experimental design, data analysis, and writing and editing the manuscript.

**References:**


**Bok, J., Bronner-Fraser, M. and Wu, D. K.** (2005). Role of the hindbrain in dorsoventral but not anteroposterior axial specification of the inner ear. *Development* **132**, 2115-2124.

**Bok, J., Brunet, L. J., Howard, O., Burton, Q. and Wu, D. K.** (2007b). Role of hindbrain in inner ear morphogenesis: analysis of Noggin knockout mice. *Dev Biol* **311**, 69-78.

**Bok, J., Dolson, D. K., Hill, P., Ruther, U., Epstein, D. J. and Wu, D. K.** (2007a). Opposing gradients of Gli repressor and activators mediate Shh signaling along the dorsoventral axis of the inner ear. *Development* **134**, 1713-1722.

**Briscoe, J. and Novitch, B. G.** (2008). Regulatory pathways linking progenitor patterning, cell fates and neurogenesis in the ventral neural tube. *Philos Trans R Soc Lond B Biol Sci* **363**, 57-70.

**Brown, A. S. and Epstein, D. J.** (2011). Otic ablation of smoothened reveals direct and indirect requirements for Hedgehog signaling in inner ear development. *Development* **138**, 3967-3976.

**Brown, S. T., Wang, J. and Groves, A. K.** (2005). Dlx gene expression during chick inner ear development. *J Comp Neurol* **483**, 48-65.

**Chang, W., Lin, Z., Kulessa, H., Hebert, J., Hogan, B. L. and Wu, D. K.** (2008). Bmp4 is essential for the formation of the vestibular apparatus that detects angular head movements. *PLoS Genet* **4**, e1000050.

**Chang, W., Nunes, F. D., De Jesus-Escobar, J. M., Harland, R. and Wu, D. K.** (1999). Ectopic noggin blocks sensory and nonsensory organ morphogenesis in the chicken inner ear. *Dev Biol* **216**, 369-381.

**Chang, W., ten Dijke, P. and Wu, D. K.** (2002). BMP pathways are involved in otic capsule formation and epithelial–mesenchymal signaling in the developing chicken inner ear. *Dev Biol* **251**, 380-394.

**Chen, Y., Gallaher, N., Goodman, R. H. and Smolik, S. M.** (1998). Protein kinase A directly regulates the activity and proteolysis of cubitus interruptus. *Proc Natl Acad Sci U S A* **95**, 2349-2354.

**Fujimori, A., Cheng, S. L., Avioli, L. V. and Civitelli, R.** (1992). Structure-function relationship of parathyroid hormone: activation of phospholipase-C, protein kinase-A and -C in osteosarcoma cells. *Endocrinology* **130**, 29-36.

**Gangopahyay, A., Oran, M., Bauer, E. M., Wertz, J. W., Comhair, S. A., Erzurum, S. C. and Bauer, P. M.** (2011). Bone morphogenetic protein receptor II is a novel mediator of endothelial nitric-oxide synthase activation. *J Biol Chem* **286**, 33134-33140.

**Gerlach, L. M., Hutson, M. R., Germiller, J. A., Nguyen-Luu, D., Victor, J. C. and Barald, K. F.** (2000). Addition of the BMP4 antagonist, noggin, disrupts avian inner ear development. *Development* **127**, 45-54.

**Granot, J., Mildvan, A. S. and Kaiser, E. T.** (1980). Studies of the mechanism of action and regulation of cAMP-dependent protein kinase. *Archives of biochemistry and biophysics* **205**, 1-17.

**Groves, A. K. and Fekete, D. M.** (2012). Shaping sound in space: the regulation of inner ear patterning. *Development* **139**, 245-257.

**Hadrys, T., Braun, T., Rinkwitz-Brandt, S., Arnold, H. H. and Bober, E.** (1998). Nkx5-1 controls semicircular canal formation in the mouse inner ear. *Development* **125**, 33-39.

**Hamburger, V. and Hamilton, H. L.** (1951). A series of normal stages in the development of the chick embryo. *J Morphol* **88**, 49-92.

**Hatch, E. P., Noyes, C. A., Wang, X., Wright, T. J. and Mansour, S. L.** (2007). Fgf3 is required for dorsal patterning and morphogenesis of the inner ear epithelium. *Development* **134**, 3615-3625.

**Herbrand, H., Guthrie, S., Hadrys, T., Hoffmann, S., Arnold, H. H., Rinkwitz-Brandt, S. and Bober, E.** (1998). Two regulatory genes, cNkx5-1 and cPax2, show different responses to local signals during otic placode and vesicle formation in the chick embryo. *Development* **125**, 645-654.

**Hui, C. C. and Angers, S.** (2011). Gli proteins in development and disease. *Annu Rev Cell Dev Biol* **27**, 513-537.

**Ingham, P. W. and McMahon, A. P.** (2001). Hedgehog signaling in animal development: paradigms and principles. *Genes Dev* **15**, 3059-3087.

**Karperien, M., Lanser, P., de Laat, S. W., Boonstra, J. and Defize, L. H.** (1996). Parathyroid hormone related peptide mRNA expression during murine postimplantation development: evidence for involvement in multiple differentiation processes. *Int J Dev Biol* **40**, 599-608.

**Lee, K., Deeds, J. D. and Segre, G. V.** (1995). Expression of parathyroid hormone-related peptide and its receptor messenger ribonucleic acids during fetal development of rats. *Endocrinology* **136**, 453-463.

**Lee, Y. S. and Chuong, C. M.** (1997). Activation of protein kinase A is a pivotal step involved in both BMP-2- and cyclic AMP-induced chondrogenesis. *J Cell Physiol* **170**, 153-165.

**Lin, Z., Cantos, R., Patente, M. and Wu, D. K.** (2005). Gbx2 is required for the morphogenesis of the mouse inner ear: a downstream candidate of hindbrain signaling. *Development* **132**, 2309-2318.

**Liu, H., Margiotta, J. F. and Howard, M. J.** (2005). BMP4 supports noradrenergic differentiation by a PKA-dependent mechanism. *Dev Biol* **286**, 521-536.

**Merlo, G. R., Paleari, L., Mantero, S., Zerega, B., Adamska, M., Rinkwitz, S., Bober, E. and Levi, G.** (2002). The Dlx5 homeobox gene is essential for vestibular morphogenesis in the mouse embryo through a BMP4-mediated pathway. *Dev Biol* **248**, 157-169.

**Minina, E., Wenzel, H. M., Kreschel, C., Karp, S., Gaffield, W., McMahon, A. P. and Vortkamp, A.** (2001). BMP and Ihh/PTHrP signaling interact to coordinate chondrocyte proliferation and differentiation. *Development* **128**, 4523-4534.

**Morsli, H., Choo, D., Ryan, A., Johnson, R. and Wu, D. K.** (1998). Development of the mouse inner ear and origin of its sensory organs. *J Neurosci* **18**, 3327-3335.

**Ogawa, H., Inouye, S., Tsuji, F. I., Yasuda, K. and Umesono, K.** (1995). Localization, trafficking, and temperature-dependence of the Aequorea green fluorescent protein in cultured vertebrate cells. *Proc Natl Acad Sci U S A* **92**, 11899-11903.

**Oh, S.-H., Johnson, R. and Wu, D. K.** (1996). Differential expression of bone morphogenetic proteins in the developing vestibular and auditory sensory organs. *J Neurosci* **16**, 6463-6475.

**Ohta, S., Mansour, S. L. and Schoenwolf, G. C.** (2010). BMP/SMAD signaling regulates the cell behaviors that drive the initial dorsal-specific regional morphogenesis of the otocyst. *Dev Biol* **347**, 369-381.

**Ohta, S., Suzuki, K., Tachibana, K. and Yamada, G.** (2003). Microbubble-enhanced sonoporation: efficient gene transduction technique for chick embryos. *Genesis* **37**, 91-101.

**Ohyama, T., Mohamed, O. A., Taketo, M. M., Dufort, D. and Groves, A. K.** (2006). Wnt signals mediate a fate decision between otic placode and epidermis. *Development* **133**, 865-875.

**Pan, Y. and Wang, B.** (2007). A novel protein-processing domain in Gli2 and Gli3 differentially blocks complete protein degradation by the proteasome. *J Biol Chem* **282**, 10846-10852.

**Riccomagno, M. M., Martinu, L., Mulheisen, M., Wu, D. K. and Epstein, D. J.** (2002). Specification of the mammalian cochlea is dependent on Sonic hedgehog. *Genes Dev* **16**, 2365-2378.

**Riccomagno, M. M., Takada, S. and Epstein, D. J.** (2005). Wnt-dependent regulation of inner ear morphogenesis is balanced by the opposing and supporting roles of Shh. *Genes Dev* **19**, 1612-1623.

**Stamataki, D., Ulloa, F., Tsoni, S. V., Mynett, A. and Briscoe, J.** (2005). A gradient of Gli activity mediates graded Sonic Hedgehog signaling in the neural tube. *Genes Dev* **19**, 626-641.

**Susperregui, A. R., Vinals, F., Ho, P. W., Gillespie, M. T., Martin, T. J. and Ventura, F.** (2008). BMP-2 regulation of PTHrP and osteoclastogenic factors during osteoblast differentiation of C2C12 cells. *J Cell Physiol* **216**, 144-152.

**Taylor, S. S., Buechler, J. A. and Yonemoto, W.** (1990). cAMP-dependent protein kinase: framework for a diverse family of regulatory enzymes. *Annu Rev Biochem* **59**, 971-1005.

**Tee, J. B., Choi, Y., Shah, M. M., Dnyanmote, A., Sweeney, D. E., Gallegos, T. F., Johkura, K., Ito, C., Bush, K. T. and Nigam, S. K.** (2010). Protein kinase A regulates GDNF/RET-dependent but not GDNF/Ret-independent ureteric bud outgrowth from the Wolffian duct. *Dev Biol* **347**, 337-347.

**Wang, B., Fallon, J. F. and Beachy, P. A.** (2000). Hedgehog-regulated processing of Gli3 produces an anterior/posterior repressor gradient in the developing vertebrate limb. *Cell* **100**, 423-434.

**Wang, W., Grimmer, J. F., Van De Water, T. R. and Lufkin, T.** (2004). Hmx2 and Hmx3 homeobox genes direct development of the murine inner ear and hypothalamus and can be functionally replaced by Drosophila Hmx. *Developmental cell* **7**, 439-453.

**Wang, W., Van De Water, T. and Lufkin, T.** (1998). Inner ear and maternal reproductive defects in mice lacking the Hmx3 homeobox gene. *Development* **125**, 621-634.

**Wilson, L. C. and Trembath, R. C.** (1994). Albright's hereditary osteodystrophy. *Journal of medical genetics* **31**, 779-784.

**Wu, D. K. and Kelley, M. W.** (2012). Molecular mechanisms of inner ear development. *Cold Spring Harb Perspect Biol* **4**, a008409.

**Wu, D. K. and Oh, S.-H.** (1996). Sensory organ generation in the chick inner ear. *J Neurosci* **16**, 6454-6462.

**Zou, H., Wieser, R., Massague, J. and Niswander, L.** (1997). Distinct roles of type I bone morphogenetic protein receptors in the formation and differentiation of cartilage. *Genes Dev* **11**, 2191-2203.

**Figures**

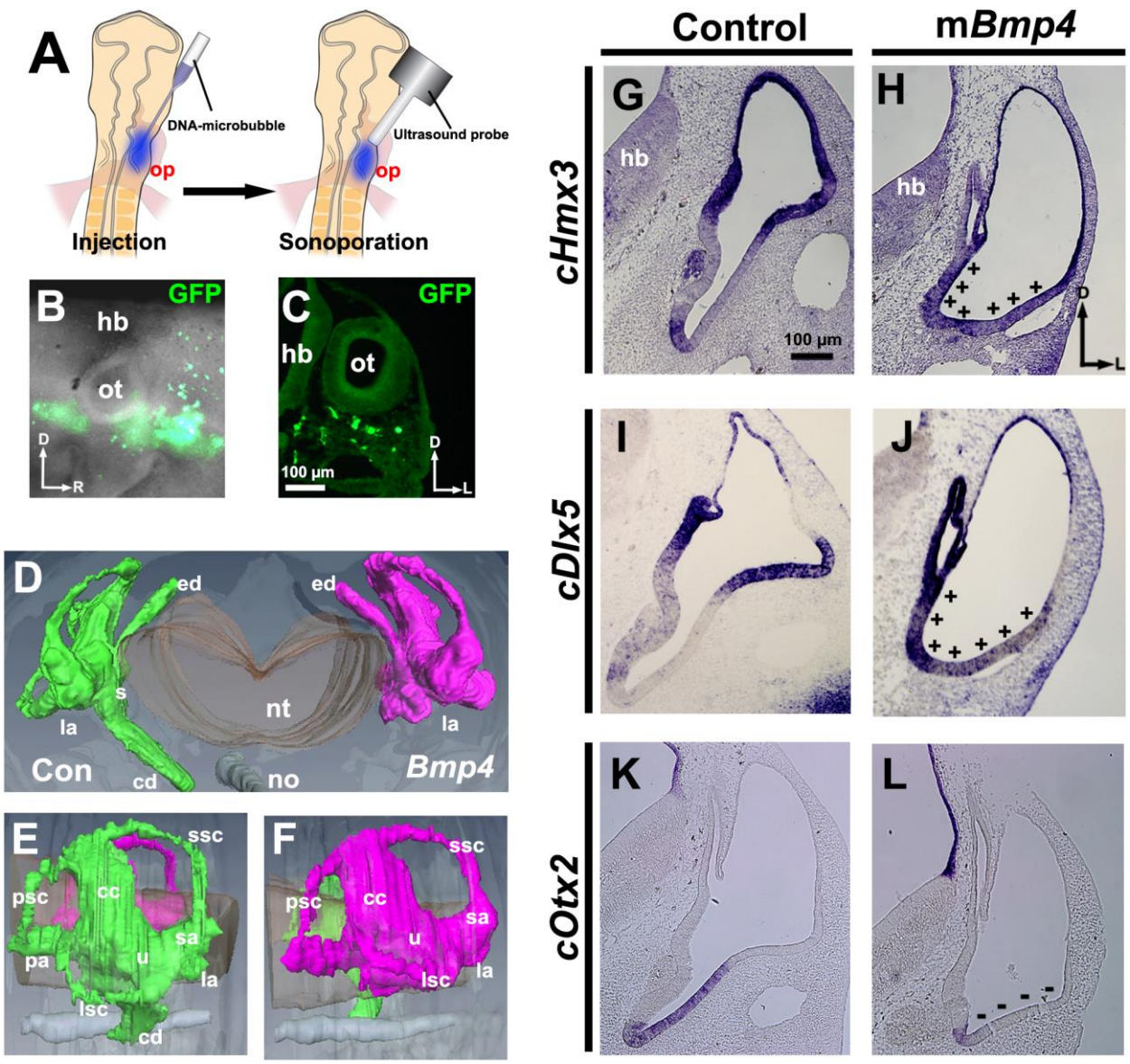


**Figure 1. *Bmp4* overexpression expands *Hmx3* and *Dlx5* expression ventrally, attenuates *Otx2* expression, and blocks formation of the cochlea.**

(**A-C**) Transfection scheme: **(A)** Diagram showing sonoporation targeted to transfect head mesenchymal cells ventral to the otic placode. (**B**) Whole-mount view 12-18 hours after sonoporation of *Gfp*. (**C**) Transverse section through another transfected embryo. D: dorsal, L: lateral, R: rostral, hb: hindbrain, op: otic placode, ot: otocyst. (**D-F**) Reconstruction (**D,** frontal view; **E,F**, lateral views) of serial transverse sections of inner ears (HH stage 30) collected after sonoporation of *Bmp4* (green: control ear, Con; magenta: experimental ear,

*Bmp4* overexpressed). cc: common crus, cd: cochlear duct, ed: endolymphatic duct, la: lateral ampulla, lsc: lateral semicircular canal, no: notochord, nt: neural tube, pa: posterior ampulla, psc: posterior semicircular canal, s: saccule, sa: superior ampulla, ssc: superior semicircular canal, u: utricle. Paint fills, n = 3; paraffin serial sections, n = 5; reconstruction, n = 1. (**G-L**) In situ hybridization of transverse sections of otocysts collected after transfection when embryos reached HH stages 24-25. D: dorsal, L: lateral, hb: hindbrain. (**G**,**H**) c*Hmx3* expression; +'s: region of expanded c*Hmx3* expression; n = 6/6, control otocysts/experimental otocysts, here and in subsequent figures). (**I**,**J**) c*Dlx5* expression; +'s: region of expanded c*Dlx5* expression; n = 9/9. (**K**,**L**) c*Otx2* expression; –'s: region of reduced c*Otx2* expression; n = 6/6. The right-left axis of histological images and reconstructions are oriented here and subsequently to align with the experimental schema, simplifying data interpretation.

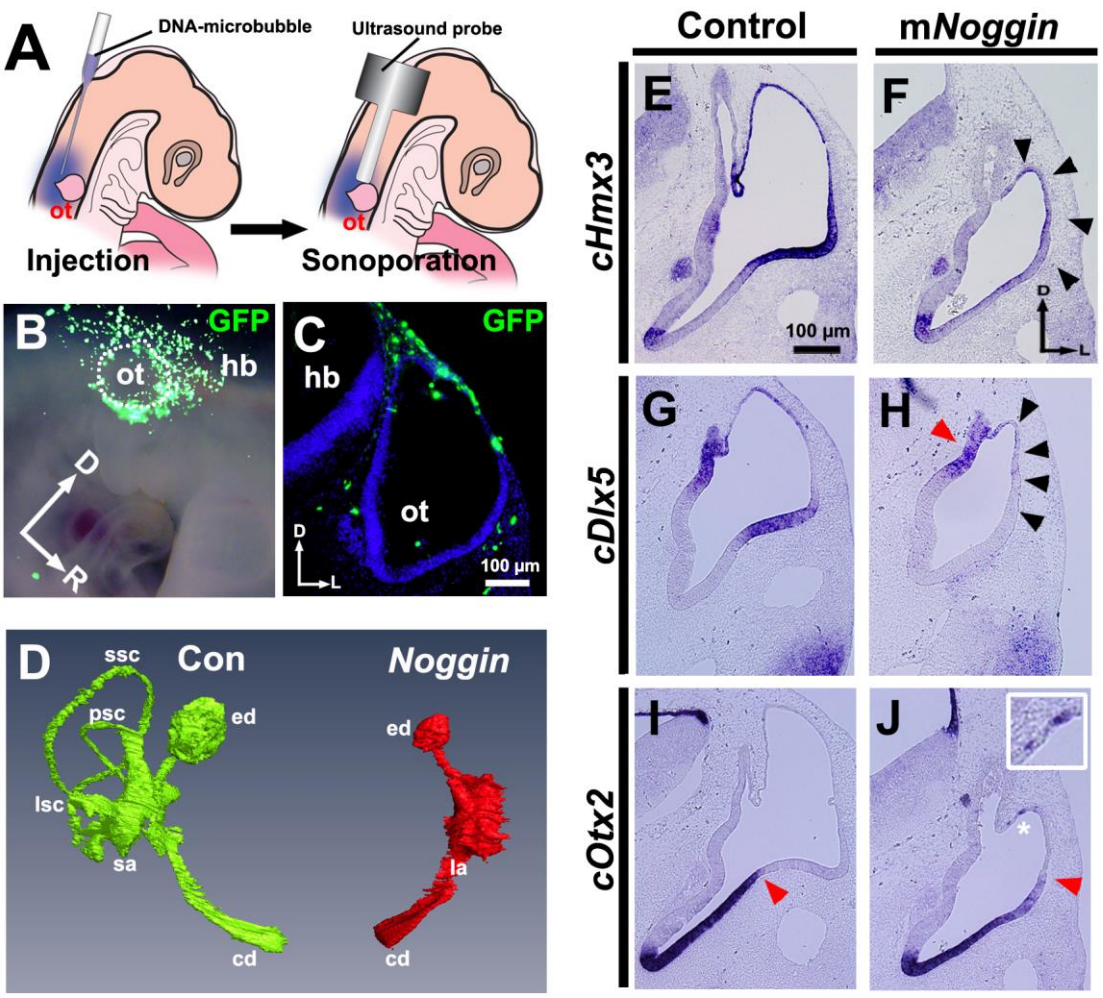


**Figure 2. *Noggin* overexpression attenuates *Hmx3* and *Dlx5* expression, expands *Otx2* expression dorsally, and blocks formation of the semicircular canals.**

(**A-C**) Transfection scheme: (**A**) Diagram showing sonoporation targeted to transfect head mesenchymal cells overlying the dorsal otocyst. (**B**) Whole-mount view 12-18 hours after sonoporation of *Gfp*. The borders of the otocyst are indicated by white dots. (**C**) Transverse section through another transfected embryo. D: dorsal, L: lateral, R: rostral, hb: hindbrain, ot: otocyst. (**D**) Frontal view of a reconstruction of serial transverse sections of inner ears at HH stage 35 collected after sonoporation of *Noggin* (green: control, Con; red: *Noggin* overexpression). Abbreviations as in Figure 1D-F. Paint fills, n = 3; paraffin serial sections, n = 3; reconstruction, n = 1. (**E-J**) In situ hybridization of transverse sections of otocysts collected after transfection when embryos reached HH stages 24-25. D: dorsal, L: lateral. (**E**,**F**) c*Hmx3* expression; arrowheads: region of reduced c*Hmx3* expression; n = 6/6. (**G**,**H**) c*Dlx5* expression; black arrowheads: region of abolished c*Dlx5* expression; red arrowhead: region (developing endolymphatic duct) of persisting c*Dlx5* expression; n = 6/6. (**I**,**J**) c*Otx2*

expression; asterisk: ectopic expression of *cOtx2*, which is enlarged in box; red arrowhead: most dorsolateral extent of *cOtx2* expression, which is expanded more dorsally after *Noggin* overexpression; n = 6/6.

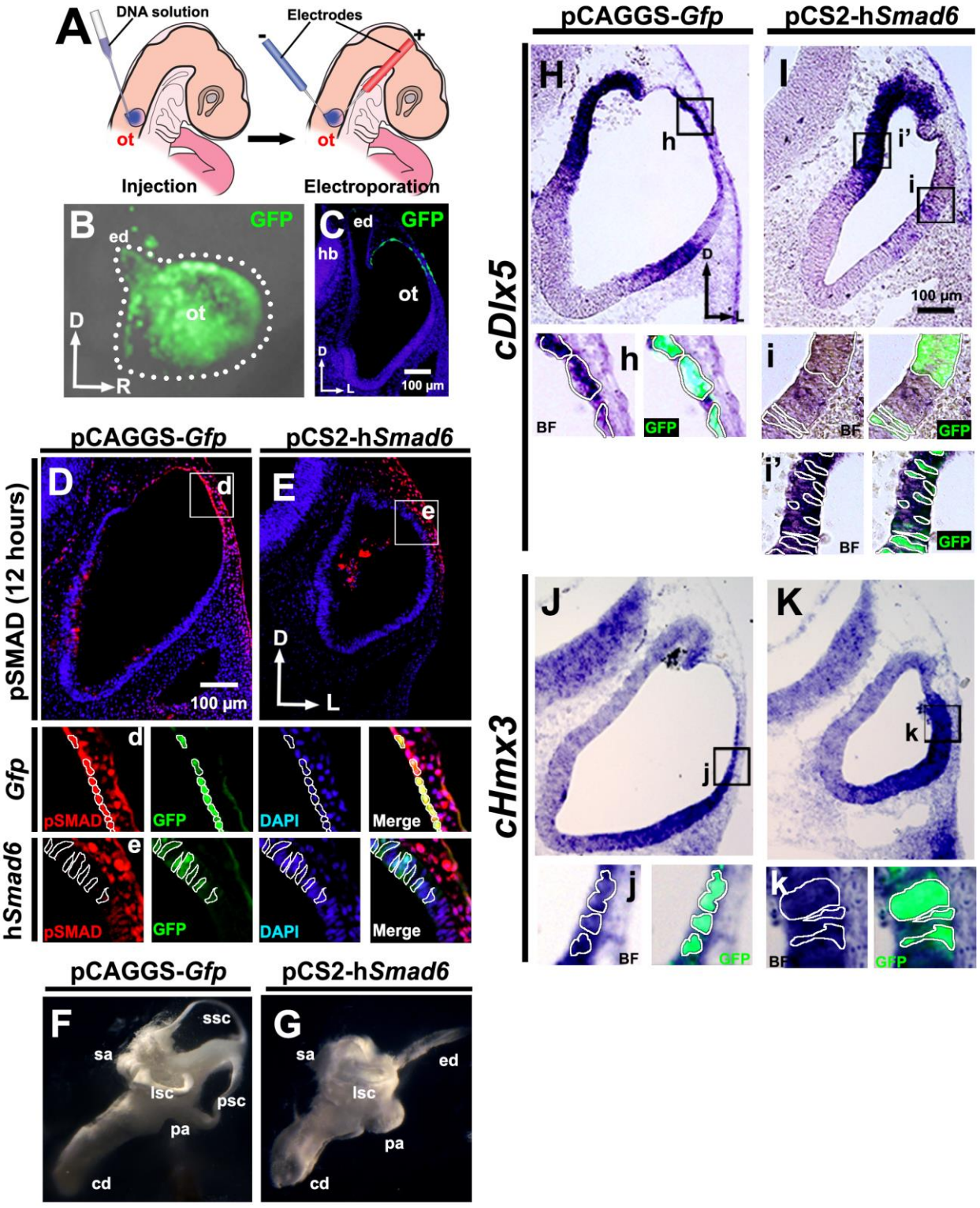


**Figure 3.** ***Smad6*** **overexpression inhibits** ***Dlx5*** **expression in the dorsolateral otocyst, but not in the dorsomedial otocyst, fails to inhibit** ***Hmx3*** **expression, and blocks formation of the semicircular canals.**

(**A-C**) Transfection scheme: (**A**) Diagram showing electroporation targeted to the dorsolateral otocyst. (**B**) Whole-mount view 12-18 hours after electroporation of *Gfp*. The borders of the otocyst are indicated by white dots. (**C**) Transverse section of the same embryo shown in (**B**). D: dorsal, L: lateral, R: rostral, ed: endolymphatic duct, hb: hindbrain, ot: otocyst. (**D,E**) pSMAD labeling of chick otocyst sections collected after electroporation. Boxes show regions enlarged below; borders of selected cells are outlined; n = 6/6. (**F**,**G**) Paint fills of chick inner ear at HH stage 30. Abbreviations as in Figure 1D-F. Paint fills, n = 5; paraffin serial sections, n = 1. (**H-K**) In situ hybridization of otocysts in transverse sections collected after transfection when embryos reached HH stages 20-21. D: dorsal, L: lateral. Boxes show regions enlarged below; borders of selected cells are outlined. (**H**,**I**) c*Dlx5* expression; ; n = 11/11. (**J**,**K**) c*Hmx3* expression; n = 6/6.

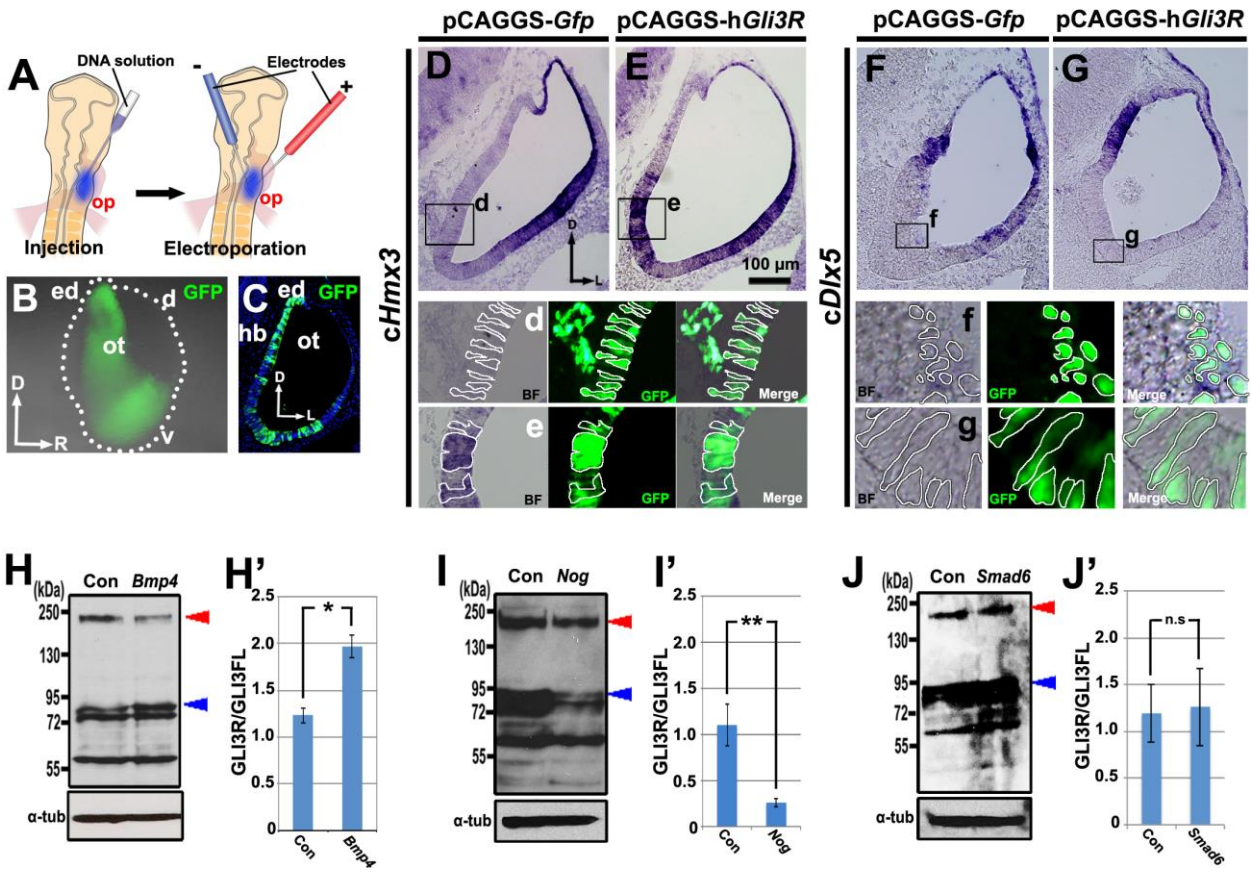


**Figure 4. *Gli3R* overexpression induces ectopic expression of *Hmx3*, but not of *Dlx5*, and increasing and decreasing BMP signaling alters the GLI3R/GLI3FL ratio in opposite directions.**

(**A-C**) Transfection scheme for Figures 4D-G, J, J': (**A**) Diagram showing electroporation into the ventral otic placode to target the ventromedial otocyst. (**B**) Whole-mount view 18-24 hours after electroporation of *Gfp*. The borders of the otocyst are indicated by white dots. (**C**) Transverse section of the same embryo shown in (**B**). D: dorsal, L: lateral, R: rostral, d: dorsal, v: ventral, ed: endolymphatic duct, hb: hindbrain, op: otic placode, ot: otocyst. (**D-G**) In situ hybridization of transverse sections of otocysts collected after transfection when embryos reached HH stages 20-21. D: dorsal, L: lateral. Boxes show regions enlarged below; borders of selected cells are outlined. (**D**,**E**) c*Hmx3* expression; n = 5/5. (**F**,**G**) c*Dlx5* expression; n = 6/6. (**H-J'**) Western blots and graphs of mean GLI3R/GLI3FL ratios in whole chick otocysts collected at the desired stage after overexpression of *Gfp* (Con) or *Bmp4* (n = 5/5), *Noggin* (n = 5/5), or *Smad6* (n = 5/5); blue arrowhead: GLI3R; red arrowhead: GLI3FL; tub: tubulin. Otocysts in (**H,H'**) were from embryos transfected as in Figure 1A, and those in

(**I,I'**) were from embryos transfected as in Figure 2A. In graphs, single asterisk: $P < 0.05$; double asterisks: $P < 0.01$; n.s.: not statistically significant.

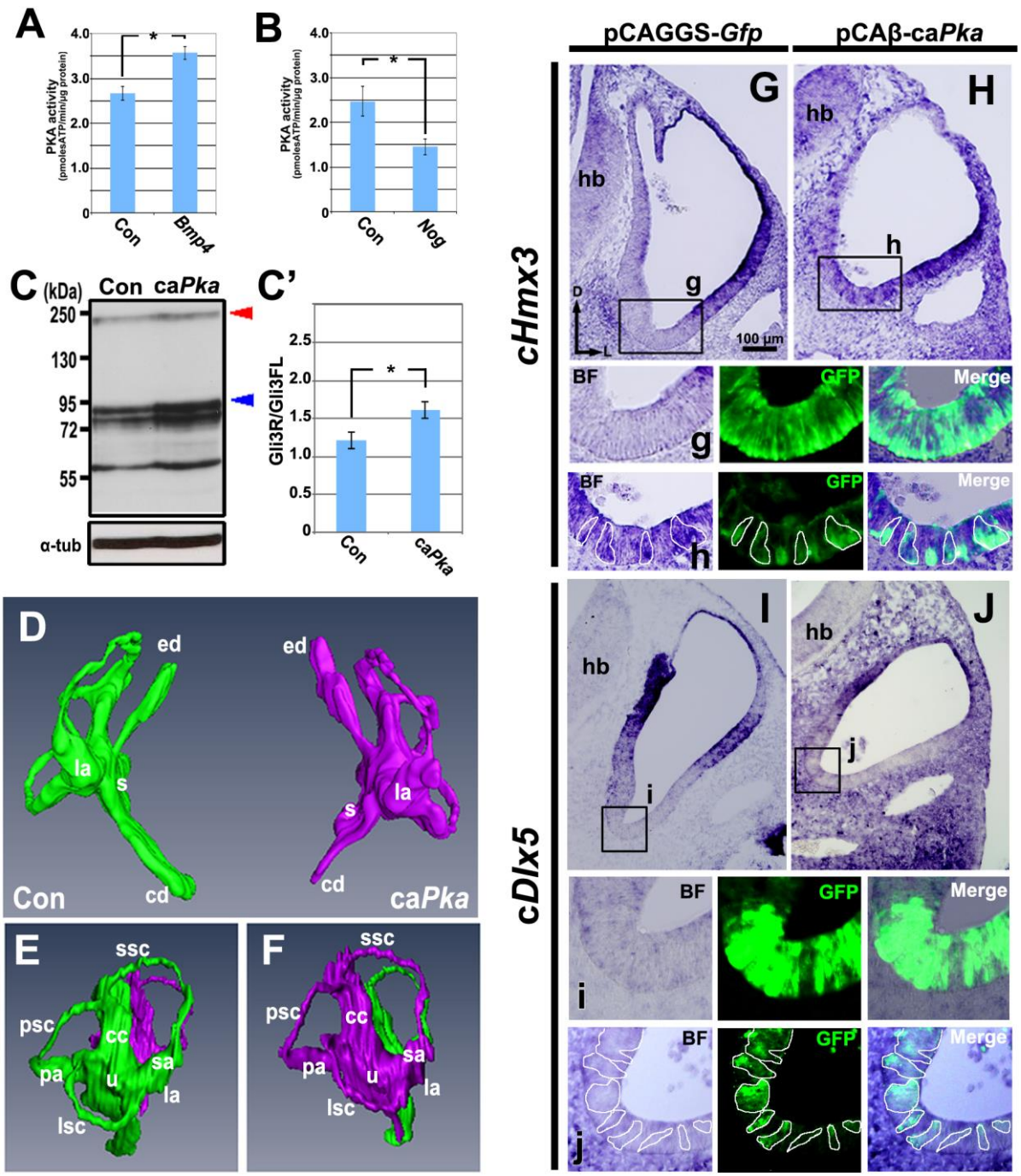


**Figure 5. Increasing and decreasing BMP signaling alters PKA activity in opposite directions, and ca*Pka* overexpression induces ectopic expression of *Hmx3*—but not of *Dlx5*—and inhibits formation of the cochlea.**

**(A**, **B)** Graphs of the mean levels of PKA activity in whole chick otocysts at HH stages 24-25 collected after overexpression of *Bmp4* (transfected as in Fig. 1A; n = 5) or *Noggin* (*Nog*) (transfected as in Fig. 1A; n = 5), compared with controls (Con). Asterisk: $P < 0.05$. (**C**, **C'**) Western blot and graph of mean GLI3R/GLI3FL ratios in whole chick otocysts at HH stages

20-21 collected after overexpression of ca*Pka* (transfected as in Fig. 4A; n = 5), compared with controls (Con). Blue arrowhead: GLI3R; red arrowhead: GLI3FL; tub: tubulin. In the graph, asterisk: $P < 0.05$. (**D-F**) Reconstruction (**D**, frontal view; **E,F**; lateral views) of serial transverse sections of inner ears at HH stage 30 (transfected as in Fig. 4A; green: control ear; Con; magenta: experimental ear; ca*Pka* overexpression). Abbreviations as in Figure 1D-F. Paraffin serial sections, n = 7; reconstruction, n = 1. (**G-J**) In situ hybridization of transverse sections of otocysts collected after transfection when embryos reached HH stages 20-21 (transfected as in Fig. 4A). D: dorsal, L: lateral. Boxes show regions enlarged below; borders of selected cells are outlined. (**G**,**H**) c*Hmx3* expression; n = 6/6. (**I**,**J**) c*Dlx5* expression; boxes show regions enlarged below; borders of selected cells are outlined; n = 2/2.

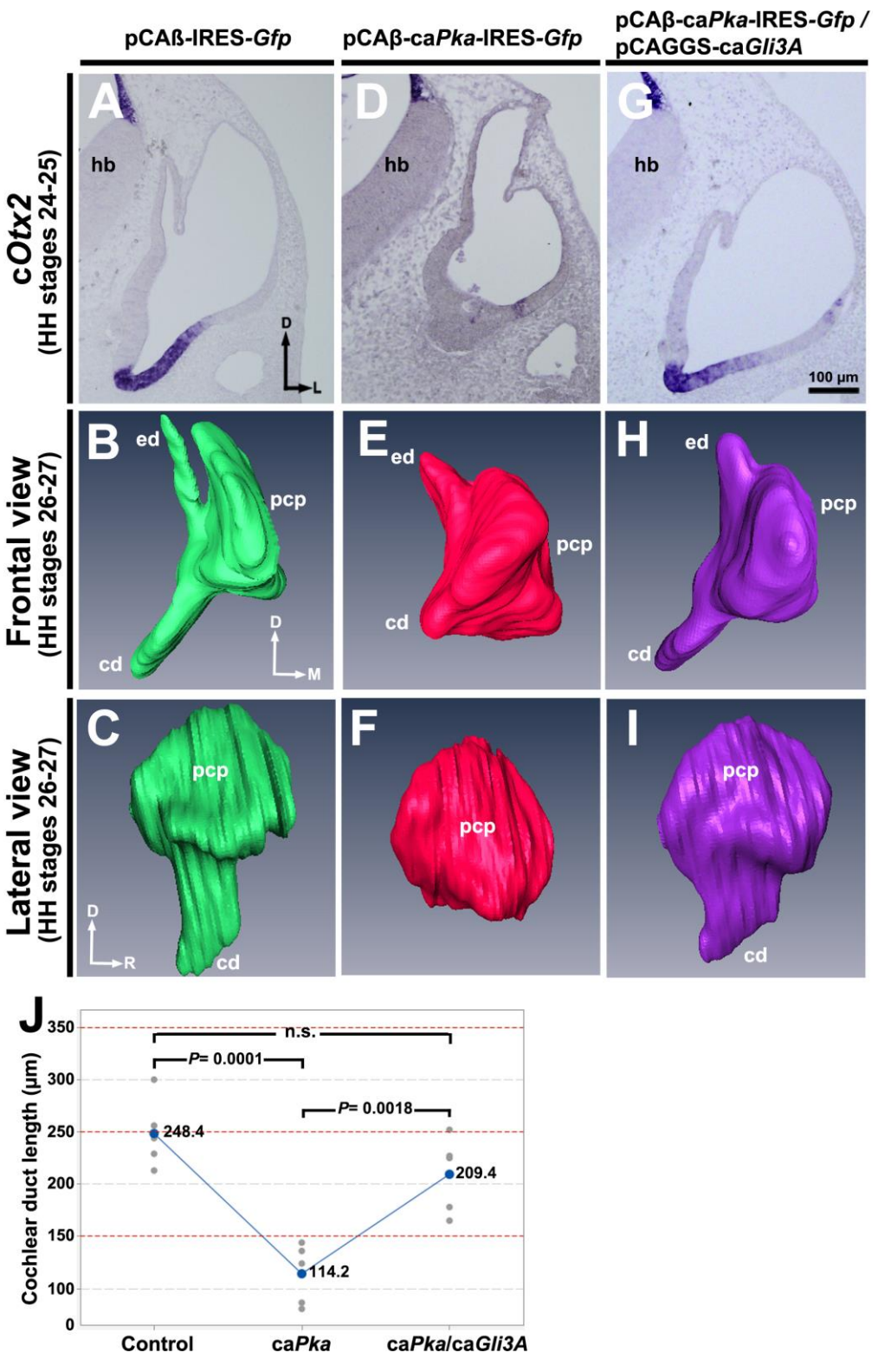

**Figure 6. ca*Gli3A* rescues ventral otocyst development arrested by caPKA.**

(**A, D, G**) In situ hybridization of transverse sections with *Otx2* after electroporation with vector alone (n = 5/5), ca*Pka* (n = 5/5), or ca*Pk*a and ca*Gli3A* (n = 5/5). D: dorsal, L: lateral, M: medial, R: rostral, hb, hindbrain. (**B-I**) Reconstructions of serial transverse sections of developing chick inner ears collected after electroporation and shown in frontal (**B, E, H**) and lateral (**C, F, I**) views. pcp, primordial canal pouch; other abbreviations as in Figure 1D-F. For each of the three groups of otocysts, paraffin serial sections, n = 4; reconstruction, n = 1. **(J)** Graph of cochlear duct length in control and transfected otocysts. n = 5 in each of the three groups.

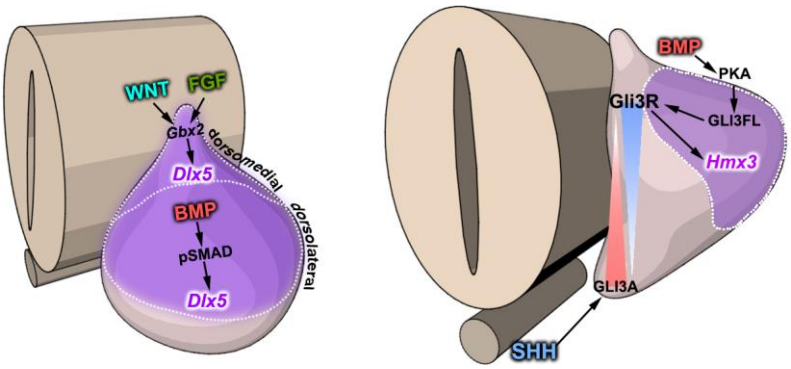


**Figure 7. Model showing the secreted factors and molecular pathways regulating otocyst DV patterning. (A)** Lateral view. (**B**) Right, oblique cross-sectional view. Some of these factors (FGFs) are secreted by cells in tissues surrounding the otocyst (e.g., head mesenchyme), whereas others (WNTs and BMPs) are secreted by cells in the otocyst wall and surrounding tissues (e.g., dorsal spinal cord).